Titre: Title:	Generalized Brewster effect using bianisotropic metasurfaces
Auteurs: Authors:	Guillaume Lavigne, & Christophe Caloz
Date:	2021
Type:	Article de revue / Article
Référence: Citation:	Lavigne, G., & Caloz, C. (2021). Generalized Brewster effect using bianisotropic metasurfaces. Optics Express, 29(7), 11361-11370. https://doi.org/10.1364/oe.423078

Titre de la revue: Journal Title:	Optics Express (vol. 29, no. 7)
Maison d'édition: Publisher:	Optica Publishing Group
URL officiel: Official URL:	https://doi.org/10.1364/oe.423078
Mention légale: Legal notice:	© 2021 Optical Society of America under the terms of the OSA Open Access Publishing Agreement

Research Article | Vol. 29, No. 7 / 29 March 2021 / Optics Express 11361
Optics EXPRESS

Generalized Brewster effect using bianisotropic metasurfaces

GUILLAUME LAVIGNE[1,*] AND CHRISTOPHE CALOZ[2]

[1] Electrical Engineering, Polytechnique Montréal, Montréal H3T 1J4, Canada
[2] Faculty of Engineering Science, KU Leuven, Leuven 3000, Belgium
[*] guillaume.lavigne@polymtl.ca

Abstract: We show that a properly designed bianisotropic metasurface placed at the interface between two arbitrary different media, or coating a dielectric medium exposed to the air, provides Brewster (reflectionless) transmission at arbitrary angles for both the TM and TE polarizations. We present a rigorous derivation of the corresponding surface susceptibility tensors based on the generalized sheet transition conditions and demonstrate by full-wave simulations the system with planar microwave metasurfaces designed for polarization-independent and azimuth-independent operations. The proposed bianisotropic metasurfaces provide deeply subwavelength matching solutions for initially mismatched media. The reported generalized Brewster effect represents a fundamental advance in optical technology, where it may both improve the performance of conventional components and enable the development of novel devices.

1. Introduction

The Brewster effect, which consists in the vanishment of the reflection of TM-polarized waves at the interface between two dielectric media at a specific incidence angle [1], has a history of more than 200 years. In 1808, Malus observed that unpolarized light becomes polarized upon reflection under a particular angle at the surface of water [2]. Seven years later, Brewster experimentally showed that this angle was equal to the inverse tangent of the ratio the refractives indices of the two media [3]. Another six years later, in 1821, Fresnel completed the understanding of the phenomenon using a mechanical model of the interface system and derived the eponymic reflection and transmission coefficients [4], which embed the Brewster effect. Finally, these formulas were generalized to magneto-electric materials, which support either TM-polarization or TE-polarization Brewster transmission, with both possible only for normal incidence, by Giles and Wild [5].

The recent advent of metasurfaces has created novel opportunities to extend the Brewster effect. Metasurfaces allow indeed unprecedented manipulations of electromagnetic waves [6,7]; specifically, bianisotropic metasurfaces [8] may produce full polarization transformation [9], anomalous reflection [10] and diffractionless generalized refraction [11,12]. They have recently been shown to support Brewster-like, i.e., reflection-less, transmission when surrounded at both sides by air in planar optical silicon nanodisk configuration [13], high-refractive-index nanorod metasurfaces [14], non-planar microwave split-ring resonator configuration [15,16] and all-angle Brewster transmission in a terahertz metasurface [17]. Moreover, they have been demonstrated to allow general Brewster transmission, i.e., between two different media, in the particular case of normal incidence in a non-planar bianisotropic loop-dipole configuration [18].

Here, following our initial suggestion in [19], we present a generalization of the Brewster effect between two arbitrary different media, for arbitrary incidence angle and arbitrary polarization, using a planar bianisotropic metasurface. We derive synthesis formulas of the corresponding metasurface susceptibility tensors and demonstrate the generalized Brewster angle by full-wave electromagnetic simulation.

#423078 https://doi.org/10.1364/OE.423078
Journal © 2021 Received 18 Feb 2021; revised 21 Mar 2021; accepted 21 Mar 2021; published 26 Mar 2021

Optics EXPRESS

2. Generalized Brewster effect

Figure 1 shows the proposed metasurface-based generalized Brewster effect. Figure 1(a) illustrates the suppression of reflection for arbitrary wave incidence angle and arbitrary polarization, Figure 1(b) defines the corresponding problem in the plane of scattering, and Figure 1(c) depicts the metaparticule used in the paper as a proof of concept in the microwave regime. The metasurface is assumed to suppress reflection without altering the direction of refraction prescribed by the Snell law for the initial pair of media and without inducing any gyrotropy (polarization rotation), while being passive, lossless and reciprocal. The preservation of the Snell law for the transmitted wave implies a uniform (without phase gradient) metasurface, and hence a uniformly periodic metastructure.

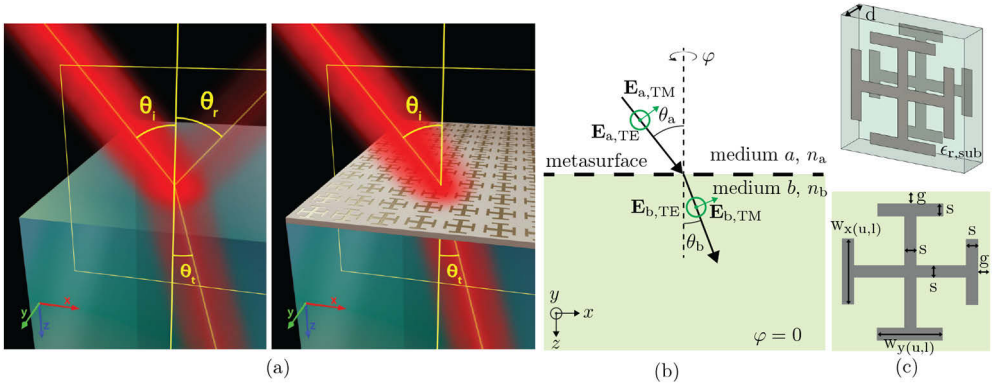

Fig. 1. Metasurface-based generalized Brewster refraction between two media. (a) Scattering of a wave impinging on the interface under an arbitrary angle (θ_a), with conventional Fresnel transmission and reflection for the case of the bare interface (left) and with reflectionless (Brewster) transmission when a properly designed metasurface is placed at the interface (right). (b) Brewster metasurface problem, for TE and TM polarizations, in the xz-plane scattering plane. (c) Proposed 2-layer conducting cross-potent metaparticle for a microwave proof of concept.

3. Susceptibility tensor derivation

3.1. Field specifications

We consider the metasurface problem depicted in Figure 1(b), where a wave incident from the medium a in the $xz-$plane at an arbitrary angle θ_a is fully transmitted, without reflection ($R = 0$), into the medium b, at the Snell angle $\theta_b = \arcsin(\frac{n_a}{n_b}\sin\theta_a)$. We assume the time-harmonic complex convention $\exp(-i\omega t)$ through the paper, and we shall apply the metasurface synthesis technique described in [20,21] to determine the susceptibility tensors of the metasurface.

The first step in the synthesis is to define the desired tangential fields at both sides of the metasurface in the plane $z = 0$. For a TM-polarized wave, these fields read

$$\mathbf{E}_{\|a,\mathrm{TM}} = \cos\theta_a e^{-ik_x x}\hat{x}, \tag{1a}$$

$$\mathbf{H}_{\|a,\mathrm{TM}} = \frac{e^{-ik_x x}}{\eta_a}\hat{y}, \tag{1b}$$

$$\mathbf{E}_{\|b,\mathrm{TM}} = T\cos\theta_b e^{-ik_x x}e^{i\phi_{\mathrm{TM}}}\hat{x}, \tag{1c}$$

$$\mathbf{H}_{\|b,\mathrm{TM}} = T\frac{e^{-ik_x x}}{\eta_b}e^{i\phi_{\mathrm{TM}}}\hat{y}, \tag{1d}$$

Optics EXPRESS

while for a TE-polarized wave, they read

$$\mathbf{E}_{\|a,\mathrm{TE}} = -e^{-ik_x x}\hat{y}, \tag{2a}$$

$$\mathbf{H}_{\|a,\mathrm{TE}} = \cos\theta_\mathrm{a}\frac{e^{-ik_x x}}{\eta_\mathrm{a}}\hat{x}, \tag{2b}$$

$$\mathbf{E}_{\|b,\mathrm{TE}} = -Te^{-ik_x x}e^{i\phi_\mathrm{TE}}\hat{y} \tag{2c}$$

$$\mathbf{H}_{\|b,\mathrm{TE}} = T\cos\theta_\mathrm{b}\frac{e^{-ik_x x}}{\eta_\mathrm{b}}e^{i\phi_\mathrm{TE}}\hat{x}, \tag{2d}$$

where k_x is the (continuous) tangential wavenumber, $\eta_{(a,b)}$ is the wave impedance in medium (a, b), and T is the transmission coefficient between the two media. The phase terms $e^{i\phi_\mathrm{TM,TE}}$ in the transmitted fields are introduced here to account for the typical phase shifts imparted to the wave by a pratical metasurface and to provide degrees of freedom that may be advantageous in the design of the unit-cell metaparticle. In these relations, T must be properly chosen to provide total transmission across the metasurface. It is obtained by enforcing power conservation across the metasurface (passivity and losslessness assumptions), i.e., by enforcing the continuity of the normal component of the Poynting vector at $z = 0$ [21]. This leads, using the fields in (1) and (2), to

$$T = \sqrt{\frac{\eta_\mathrm{b}\cos\theta_\mathrm{a}}{\eta_\mathrm{a}\cos\theta_\mathrm{b}}}, \tag{3}$$

which is identical for the TE and TM polarizations.

3.2. Transition conditions

The boundary conditions in the plane of the metasurface ($z = 0$) are the generalized sheet transition conditions [7,20,21]

$$\hat{z}\times\Delta\mathbf{H} = i\omega\epsilon\overline{\overline{\chi}}_\mathrm{ee}\mathbf{E}_\mathrm{av} + i\omega\overline{\overline{\chi}}_\mathrm{em}\sqrt{\mu\epsilon}\mathbf{H}_\mathrm{av}, \tag{4a}$$

$$\Delta\mathbf{E}\times\hat{z} = i\omega\mu\overline{\overline{\chi}}_\mathrm{me}\sqrt{\frac{\epsilon}{\mu}}\mathbf{E}_\mathrm{av} + i\omega\mu\overline{\overline{\chi}}_\mathrm{mm}\mathbf{H}_\mathrm{av}, \tag{4b}$$

where the symbol Δ and the subscript 'av' represent the differences and averages of the tangential fields at both sides of the metasurface, i.e.,

$$\Delta\mathbf{\Phi} = \mathbf{\Phi}_b - \mathbf{\Phi}_a, \tag{5}$$

$$\mathbf{\Phi}_\mathrm{av} = (\mathbf{\Phi}_a + \mathbf{\Phi}_b)/2, \tag{6}$$

where $\mathbf{\Phi} = \mathbf{E}, \mathbf{H}$, and $\overline{\overline{\chi}}_\mathrm{ee}$, $\overline{\overline{\chi}}_\mathrm{em}$, $\overline{\overline{\chi}}_\mathrm{me}$ and $\overline{\overline{\chi}}_\mathrm{mm}$ are the bianisotropic surface susceptibility tensors describing the metasurface. In this paper, we shall restrict our attention to purely tangential susceptibility metasurfaces, corresponding to 2×2 tensors and hence 16 susceptibility parameters in Eq. (4), although metasurfaces involving normal susceptibility components may offer further possibilities [21], as will be discussed later.

3.3. Homoanisotropic metasurface

We heuristically start our quest for the design described in connection with Figure 1 by considering the simplest type of metasurface, namely an homoanisotropic metasurface, which is defined as a metasurface whose only nonzero susceptibility tensors are $\overline{\overline{\chi}}_\mathrm{ee}$ and $\overline{\overline{\chi}}_\mathrm{mm}$. The nongyrotropy condition implies then $\chi_\mathrm{ee}^{xy} = \chi_\mathrm{ee}^{yx} = \chi_\mathrm{mm}^{xy} = \chi_\mathrm{mm}^{yx} = 0$ [21], which decouples the two polarizations with χ_ee^{xx} and χ_mm^{yy} for TM and χ_ee^{yy} and χ_mm^{xx} for TE (see Figure 1(b)). Inserting the specifications

Optics EXPRESS

(1) and (2) into the field differences and averages (5) and (6), substituting the resulting expressions into into (4), and solving for the four nonzero susceptibility components yields

$$\chi_{\mathrm{ee}}^{xx} = \frac{2i\eta_{\mathrm{a}}Te^{i\phi_{\mathrm{TM}}} - 2i\eta_{\mathrm{b}}}{\eta_{\mathrm{a}}\eta_{\mathrm{b}}\omega\epsilon_0\cos\theta_{\mathrm{a}} + \eta_{\mathrm{a}}\eta_{\mathrm{b}}T\omega\epsilon_0 e^{i\phi_{\mathrm{TM}}}\cos\theta_{\mathrm{b}}}, \tag{7a}$$

$$\chi_{\mathrm{mm}}^{yy} = -\frac{2i\eta_{\mathrm{a}}\eta_{\mathrm{b}}\left(\cos\theta_{\mathrm{a}} - Te^{i\phi_{\mathrm{TM}}}\cos\theta_{\mathrm{b}}\right)}{\mu_0\omega\left(\eta_{\mathrm{b}} + \eta_{\mathrm{a}}Te^{i\phi_{\mathrm{TM}}}\right)}. \tag{7b}$$

$$\chi_{\mathrm{ee}}^{yy} = \frac{2i\eta_{\mathrm{a}}Te^{i\phi_{\mathrm{TE}}}\cos\theta_{\mathrm{b}} - 2i\eta_{\mathrm{b}}\cos\theta_{\mathrm{a}}}{\eta_{\mathrm{a}}\eta_{\mathrm{b}}\omega\epsilon_0 + \eta_{\mathrm{a}}\eta_{\mathrm{b}}T\omega\epsilon_0 e^{i\phi_{\mathrm{TE}}}}, \tag{8a}$$

$$\chi_{\mathrm{mm}}^{xx} = \frac{i\eta_{\mathrm{a}}\eta_{\mathrm{b}}\left(-1 + Te^{i\phi_{\mathrm{TE}}}\right)}{-\eta_{\mathrm{b}}\mu_0\omega\cos\theta_{\mathrm{a}} + \eta_{\mathrm{a}}\mu_0 T\omega e^{i\phi_{\mathrm{TE}}}\cos\theta_{\mathrm{b}}}. \tag{8b}$$

The complex nature of these susceptibilities indicates the presence of loss or gain, whereas we are searching for a lossless and gainless metasurface. This attempt is therefore unsuccessful, but it demonstrates the necessity for a really bianisotropic metasurface, as will be shown next.

3.4. Bianisotropic metasurface

At this point, we can still hope that adding heteroanisotropy, corresponding to the susceptibilitity tensors $\overline{\overline{\chi}}_{\mathrm{em}}$ and $\overline{\overline{\chi}}_{\mathrm{me}}$, may allow to remove the loss-gain constraint of the previous design via the resulting extra degrees of freedom. Let us thus add the two heterotropic allowed pairs of nongyrotropic components, namely χ_{em}^{xy} and χ_{me}^{yx} for TM and χ_{em}^{yx} and χ_{me}^{xy} for TE. This increases the number of parameters to eight, and implies therefore the specification of an additional wave transformation for each polarization in order to make the system of Eqs. (4) full-rank and hence the synthesis problem exactly determined. Since some forms of bianisotropy can lead to nonreciprocity [22], which is here prohibited, we shall enforce reciprocity by specifying a second wave transformation corresponding to the time-reversed version of the fields in (1) and (2) [23]. The resulting system of equations can be compactly written as

$$\begin{bmatrix} \Delta H_{y1} & \Delta H_{y2} \\ \Delta E_{x1} & \Delta E_{x2} \end{bmatrix} = \begin{bmatrix} -i\omega\epsilon_0\chi_{\mathrm{ee}}^{xx} & -ik_0\chi_{\mathrm{em}}^{xy} \\ -ik_0\chi_{\mathrm{me}}^{yx} & -i\omega\mu_0\chi_{\mathrm{mm}}^{yy} \end{bmatrix} \begin{bmatrix} E_{x1,\mathrm{av}} & E_{x2,\mathrm{av}} \\ H_{y1,\mathrm{av}} & H_{y2,\mathrm{av}} \end{bmatrix}, \tag{9}$$

for the TM polarization, and as

$$\begin{bmatrix} \Delta H_{x1} & \Delta H_{x2} \\ \Delta E_{y1} & \Delta E_{y2} \end{bmatrix} = \begin{bmatrix} -i\omega\epsilon_0\chi_{\mathrm{ee}}^{yy} & -ik_0\chi_{\mathrm{em}}^{yx} \\ -ik_0\chi_{\mathrm{me}}^{xy} & -i\omega\mu_0\chi_{\mathrm{mm}}^{xx} \end{bmatrix} \begin{bmatrix} E_{y1,\mathrm{av}} & E_{y2,\mathrm{av}} \\ H_{x1,\mathrm{av}} & H_{x2,\mathrm{av}} \end{bmatrix}, \tag{10}$$

for the TE polarization, where the subscript 1 corresponds to the fields in (1) and (2), and the subscript 2 corresponds to their time-reversed counterpart. Solving this system for the eight susceptibility components yields

$$\chi_{\mathrm{ee}}^{xx} = -\frac{8T\sin\phi_{\mathrm{TM}}}{\omega\epsilon\left(T\alpha(\eta_{\mathrm{b}}\cos\phi_{\mathrm{TM}} + \eta_{\mathrm{a}}T) + 2\cos\theta_{\mathrm{a}}(\eta_{\mathrm{b}} + \eta_{\mathrm{a}}T\cos\phi_{\mathrm{TM}})\right)}, \tag{11a}$$

$$\chi_{\mathrm{em}}^{xy} = -\chi_{\mathrm{me}}^{yx} = \frac{-2i\left(T\alpha(\eta_{\mathrm{b}}\cos\phi_{\mathrm{TM}} - \eta_{\mathrm{a}}T) + 2\cos\theta_{\mathrm{a}}(\eta_{\mathrm{b}} - \eta_{\mathrm{a}}T\cos\phi_{\mathrm{TM}})\right)}{k\left(T\alpha(\eta_{\mathrm{b}}\cos\phi_{\mathrm{TM}} + \eta_{\mathrm{a}}T) + 2\cos\theta_{\mathrm{a}}(\eta_{\mathrm{b}} + \eta_{\mathrm{a}}T\cos\phi_{\mathrm{TM}})\right)}, \tag{11b}$$

$$\chi_{\mathrm{mm}}^{yy} = -\frac{8\eta_{\mathrm{a}}\eta_{\mathrm{b}}T\cos\theta_{\mathrm{a}}\sin\phi_{\mathrm{TM}}\cos\theta_{\mathrm{b}}}{u\omega\left(T\alpha(\eta_{\mathrm{b}}\cos\phi_{\mathrm{TM}} + \eta_{\mathrm{a}}T) + 2\cos\theta_{\mathrm{a}}(\eta_{\mathrm{b}} + \eta_{\mathrm{a}}T\cos\phi_{\mathrm{TM}})\right)} \tag{11c}$$

Optics EXPRESS

for the TM polarization and

$$\chi_{\mathrm{ee}}^{yy} = \frac{8T\cos\theta_{\mathrm{a}}\sin\phi_{\mathrm{TE}}\cos\theta_{\mathrm{b}}}{\omega\epsilon\left(\eta_{\mathrm{a}}T(T+\cos\phi_{\mathrm{TE}})\alpha + 2\eta_{\mathrm{b}}\cos\theta_{\mathrm{a}}(T\cos\phi_{\mathrm{TE}}+1)\right)}, \tag{12a}$$

$$\chi_{\mathrm{em}}^{yx} = -\chi_{\mathrm{me}}^{xy} = -\frac{2i\left(\eta_{\mathrm{a}}T(T-\cos\phi_{\mathrm{TE}})\alpha + 2\eta_{\mathrm{b}}\cos\theta_{\mathrm{a}}(T\cos\phi_{\mathrm{TE}}-1)\right)}{k\left(\eta_{\mathrm{a}}T(T+\cos\phi_{\mathrm{TE}})\alpha + 2\eta_{\mathrm{b}}\cos\theta_{\mathrm{a}}(T\cos\phi_{\mathrm{TE}}+1)\right)}, \tag{12b}$$

$$\chi_{\mathrm{mm}}^{xx} = \frac{8\eta_{\mathrm{a}}\eta_{\mathrm{b}}T\sin\phi_{\mathrm{TE}}}{u\omega\eta_{\mathrm{a}}T(T+\cos\phi_{\mathrm{TE}})\alpha + 2\eta_{\mathrm{b}}\cos\theta_{\mathrm{a}}(T\cos\phi_{\mathrm{TE}}+1)} \tag{12c}$$

for the TE polarization, with $\alpha = \sqrt{\frac{2n_{\mathrm{a}}^2\cos(2\theta\mathrm{a})}{n_{\mathrm{b}}^2} - \frac{2n_{\mathrm{a}}^2}{n_{\mathrm{b}}^2} + 4}$. [21]. The direct responses – χ_{ee}^{xx}, χ_{ee}^{yy}, χ_{mm}^{xx} and χ_{mm}^{yy} – are purely real and the cross responses – χ_{em}^{xy}, χ_{em}^{yx}, χ_{me}^{xy} and χ_{me}^{yx} – are purely imaginary, which indicates that the metasurface is lossless and gainless [21] Thus, this design satisfies all the chosen requirements: it provides Brewster ($R = 0$) transmission for arbitrary incidence and polarization while being lossless and gainless, nongyrotropic and reciprocal. Hence, inserting a metasurface having the surface susceptibilities of (11) and (12) between two different media will achieve full transmission for the specified angle of incidence for the TM and TE polarizations, respectively. The realized Brewster transmission may be explained in terms of the metaparticles operating as Huygens' sources, with electric and magnetic dipole resonances that mutually couple so as to act as an impedance transformer. [18].

4. Metaparticle design

We now need to determine the shape of a metaparticle that realizes the susceptibilities in (11) and (12). This shape can be devised upon the basis of a simple pair of conducting wires, typically folded in a dog-bone shape for higher homogeneity, as shown in Fig. 2. The direct responses, χ_{ee}^{xx} and χ_{mm}^{yy}, can be realized with identical wires, as shown in Fig. 2(a). However, such a symmetric structure does not support cross responses. Such responses, specifically the required components χ_{me}^{yx} and χ_{em}^{xy}, can be obtained by breaking the symmetry of the wire-pair, as shown in Fig. 2(b). The exact values of these parameters can be obtained by tuning the level of asymmetry of the structure. Repeating this reasoning for the perpendicular polarization leads to a double dog-bone structure having the form of a cross potent, also often called Jerusalem cross in the literature on metamaterials, which provides independent tuning [24] of the four other susceptibility components – χ_{ee}^{yy}, χ_{mm}^{yy}, χ_{me}^{xy} and χ_{em}^{yx}.

The metaparticle obtained in this fashion will naturally induce some transmission phase, depending on the amounts of asymmetry, and coupling between the two layers. In the present application (Brewster transmission), this phase is not critical, and the design is therefore fully satisfactory as such. If one would wish, for some reason, to add control over the phase, an extra degree of freedom would need to be introduced in the structure. This can be typically accomplished by inserting a third conducting layer – a three-layer structure has been shown to provide full phase coverage with matching [11,12,21] – which can be designed from scattering parametric mapping [7,11,21] or using a transmission-line admittance model [12,25].

Optics EXPRESS

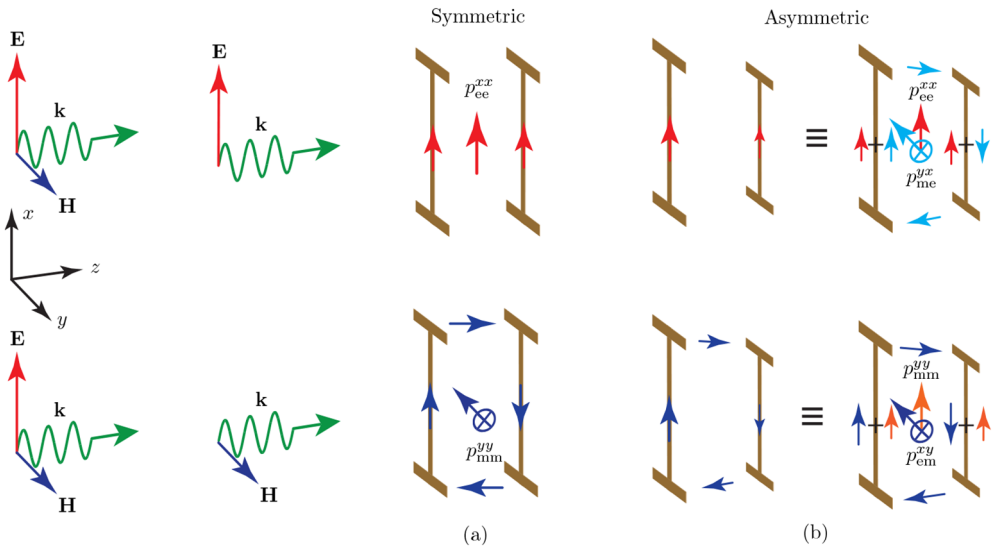

Fig. 2. Folded wire-pair metaparticle (half of the complete cross-potent metaparticle). (a) Symmetric structure, supporting only the susceptibility components, χ_{ee}^{xx} and χ_{mm}^{yy}. (b) Asymmetric structure providing the four susceptibility components required in (11). The complementary perpendicular wire pair provide the four susceptibility components required in (12). The notation p_{me}^{yx} represents the y component of the magnetic dipole response due to the x component of the electric field excitation, and so on.

5. Results

As proofs of concept, we designed a series of two-layered metasurfaces composed of cross-potent resonators, as shown in Fig. 1(c). The metasurfaces were designed and simulated using CST Studio 2019 with periodic boundary conditions.

Fig. 3 presents the results for the metasurface design with the susceptibilities (11) and (12), which correspond to polarization-independent (TE and TM) Brewster transmission in the xz-plane. These results show that the specifications are perfectly realized by the designed metasurfaces for the chosen Brewster angles (θ_a of 0°, 30° and 75°) in the X-band frequency range and also show the angular response of the metasurface system at the operating frequency of the metasurface.

The design of Fig. 3, with coinciding TM and TE Brewster angles, provides full reflection suppression for unpolarized light. However, this response is restricted to scattering in the xz ($\phi = 0$) plane. Indeed, according to Eqs. (11) and (12), we have $\chi_{ee}^{yy} \neq \chi_{ee}^{xx}$, $\chi_{mm}^{xx} \neq \chi_{mm}^{yy}$, $\chi_{em}^{xy} \neq \chi_{em}^{yx}$ and $\chi_{me}^{xy} \neq \chi_{me}^{yx}$, and therefore the metasurface structure is anisotropic since the rotation $(x, y) \rightarrow (y, -x)$ implies different susceptibilities and different susceptibility cannot lead to the same scattering response.

This single scattering plane restriction can be lifted with the same set of (eight) susceptibility parameters for one of the two polarizations (TM or TE) by combining the selected (TM or TE) xz-plane equations in (11) and (12) with the corresponding yz-plane equations obtained via the permutations $(x, y) \rightarrow (y, -x)$, which is in fact equivalent to making the structure isotropic ($\chi_{ee}^{yy} = \chi_{ee}^{xx}$, $\chi_{mm}^{xx} = \chi_{mm}^{yy}$, $\chi_{em}^{xy} = \chi_{em}^{yx}$ and $\chi_{me}^{xy} = \chi_{me}^{yx}$) since the same Brewster response is expected in the two planes for the selected polarization. The results for corresponding metasurfaces are presented in Fig. 4. They further confirm the accuracy of the proposed design.

Optics EXPRESS

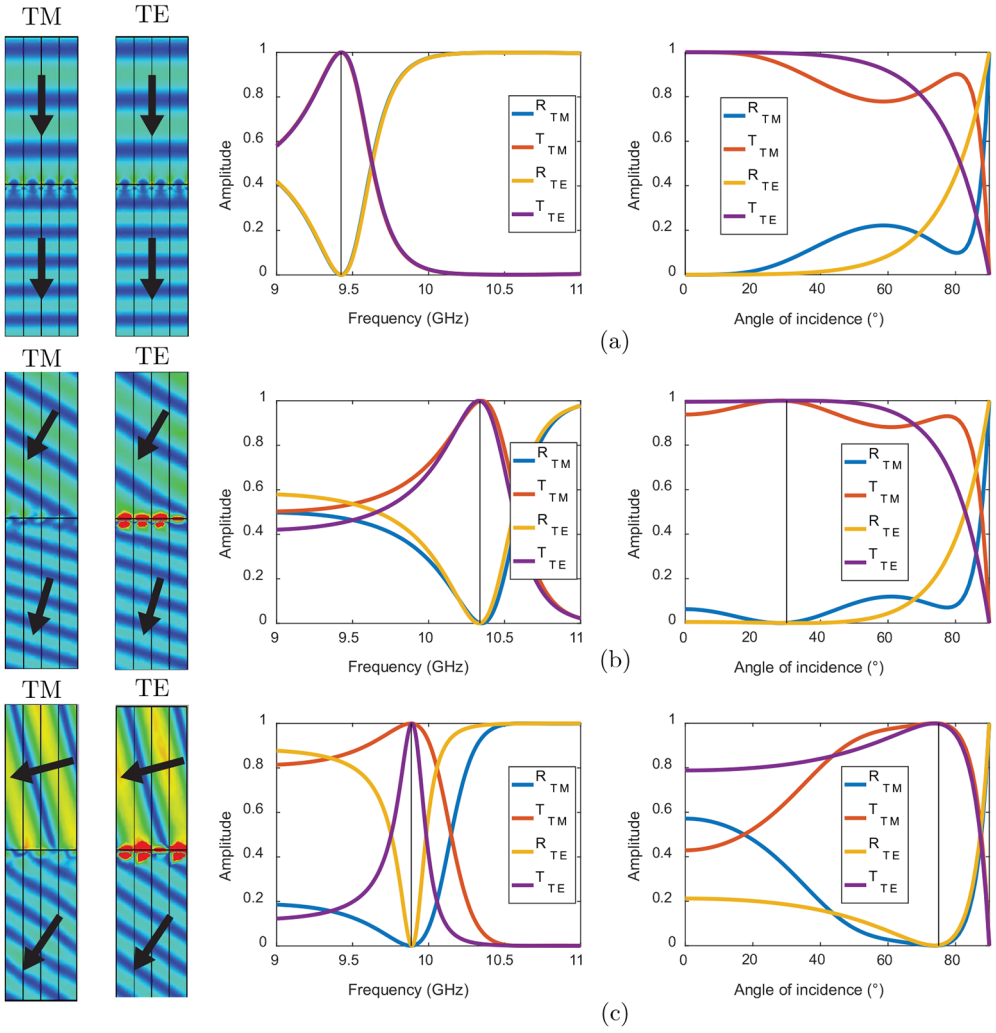

Fig. 3. Full-wave simulated electric field amplitude distribution, frequency response and angular response of the reflectance and transmittance for polarization-independent xz-plane ($\varphi = 0$) Brewster metasurfaces with the general parameters $(\epsilon_{r,a}, \epsilon_{r,b}) = (1, 3)$ (bare-interface Brewster angle for the TM polarization at 60°), $\epsilon_{r,subs} = 3$, $d = 1.52$ mm, $s = 0.5$ mm and $g = 0.5$ mm. (a) Brewster angle at $\theta_a = 0$ (normal incidence) with $w_{yu} = w_{xu} = 3.9$ mm and $w_{yl} = w_{xl} = 2.75$ mm. (b) Brewster angle at $\theta_a = 30°$ with $w_{yu} = 3.2$ mm, $w_{xu} = 3.3$ mm, $w_{yl} = 2.2$ mm and $w_{xl} = 2.2$ mm. (c) Brewster angle at $\theta_a = 75°$ with $w_{yu} = 3.35$ mm, $w_{xu} = 3.9$ mm, $w_{yl} = 2.65$ mm and $w_{xl} = 2.45$ mm.

Optics EXPRESS

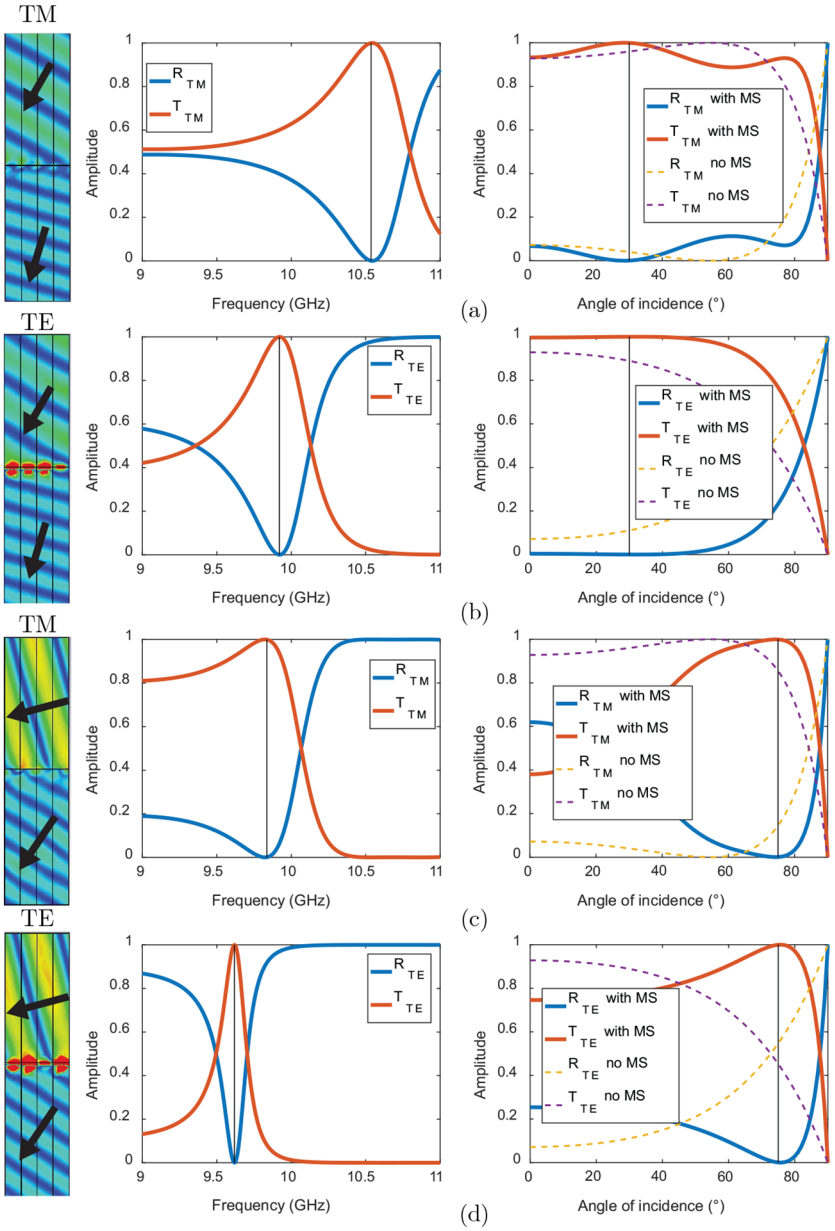

Fig. 4. Full-wave simulated electric field amplitude distribution, frequency response and angular response of the reflectance and transmittance for azimuth-independent ($\forall\varphi$) single-polarization (TM or TE) Brewster metasurfaces with the same general parameters as in Fig. 3. (a) TM-Brewster angle at $\theta_a = 30°$ with $w_{xu} = w_{yu} = 3.15$ mm and $w_{xl} = w_{yl} = 2.1$ mm. (b) TE-Brewster angle at $\theta_a = 30°$ with $w_{yu} = w_{xu} = 3.3$ mm and $w_{yl} = w_{xl} = 2.45$ mm. (c) TM-Brewster angle at $\theta_a = 75°$ with $w_{xu} = w_{yu} = 3.9$ mm and $w_{xl} = w_{yl} = 2.5$ mm. (d) TE-Brewster angle at $\theta_a = 75°$ with $w_{yu} = w_{xu} = 3.55$ mm and $w_{yl} = w_{xl} = 2.85$ mm.

Optics EXPRESS

6. Discussion

Although the eight-parameter metasurfaces considered here are restricted to either single-plane or single-polarization Brewster transmission, bianisotropic metasurfaces involving a greater number of susceptibility parameters might be able to provide universal Brewster transmission. Since the possibilities of transverse (x and y) susceptibilities have been exhausted, such metasurfaces would require resorting to normal z susceptibilities. Although the related design is in principle still analytically tractable thanks to the uniformity of the metasurface [21], it is considerably more involved and will therefore be deferred to a later study.

Equations (11) and (12) do not only provide the sought after Brewster transmission design. They point to an extra fundamental capability of an interfacing bianisotropic metasuface that occurs when $\phi_{\rm TM} = \phi_{\rm TE} = 0$, which can be achieved by phase compensation or adjustment. In this case, we have $\chi_{\rm ee}^{xx} = \chi_{\rm mm}^{yy} = \chi_{\rm ee}^{yy} = \chi_{\rm mm}^{xx} = 0$, which leads to the heteroanisotropic generalized sheet transition conditions

$$\hat{z} \times \Delta\mathbf{H} = jk\overline{\overline{\chi}}_{\rm em}\mathbf{H}_{\rm av}, \tag{13a}$$

$$\Delta\mathbf{E} \times \hat{z} = jk\overline{\overline{\chi}}_{\rm me}\mathbf{E}_{\rm av}, \tag{13b}$$

with $\overline{\overline{\chi}}_{\rm em} = -\overline{\overline{\chi}}_{\rm em}^{\rm T}$ for reciprocity [22]. The corresponding reflection coefficients can easily be computed from general field expressions [21]. They read

$$r_{\rm TM} = \frac{\eta_1 \cos\theta_1 - \eta_{2,\rm TM,eff} \cos\theta_2}{\eta_1 \cos\theta_1 + \eta_{2,\rm TM,eff} \cos\theta_2}, \tag{14a}$$

$$r_{\rm TE} = \frac{\eta_{2,\rm TE,eff} \cos\theta_1 - \eta_1 \cos\theta_2}{\eta_{2,\rm TE,eff} \cos\theta_1 + \eta_1 \cos\theta_2}, \tag{14b}$$

where

$$\eta_{2,\rm TM,eff} = \eta_2 \frac{(2i - k\chi_{\rm em}^{xy})^2}{(2i + k\chi_{\rm em}^{xy})^2}, \tag{15a}$$

$$\eta_{2,\rm TE,eff} = \eta_2 \frac{(2i - k\chi_{\rm em}^{yx})^2}{(2i + k\chi_{\rm em}^{yx})^2}. \tag{15b}$$

The relations (14) have the same mathematical form as the conventional Fresnel reflection coefficients [1]. This reveals that the proposed [medium – bianisotropic metasurface – medium] system is equivalent to a [medium – *effective medium*] system, with the effective medium having the impedances given by Eqs. (15). Thus, inserting such a bianisotropic metasurface at the interface between two media or coating a dielectric medium exposed to free space with it can change the effective bulk impedance of the transmission medium, which enriches the design possibilities of existing materials.

Although the proof of concept systems in Figs. 3 and 4 pertain to the microwave regime, where bianisotropic metasurfaces (surrounded by air) have been well documented, bianisotropic metasurfaces have also been recently demonstrated in all-dielectric configuration [26,27]. Therefore, the proposed concepts of metasurface-based generalized Brewster effective refractive medium can be readily extended to the optical regime, where they may be particularly beneficial in terms of reducing the insertion loss associated to impedance mismatch in many common components.

7. Conclusion

In summary, we have shown that a properly designed bianisotropic metasurface placed at the interface between two dielectric media or coating a dielectric medium exposed to the air provides Brewster transmission at arbitrary angles and for both the TM and TE polarizations. We

Optics EXPRESS

have presented a rigorous derivation of the corresponding surface susceptibility tensors and demonstrated the system by microwave proof-of-concept designs. Moreover, we have noted that such a system leads to the concept of effective refractive media with tailorable impedances. The proposed bianisotropic metasurfaces offer deeply subwavelength matching solutions for initially mismatched media, and alternatively lead to the possibility of on-demand manipulation of the conventional Fresnel coefficients. They represent thus a fundamental advance in optical science and posses a considerable potential for novel technological developments.

Disclosures. The authors declare no conflicts of interest.

References

1. B. E. Saleh, M. C. Teich, and B. E. Saleh, *Fundamentals of photonics*, vol. 22 (Wiley, New York, 1991).
2. É.-L. Malus, "Sur une propriété de la lumière réfléchie," Mem. Phys. Chim. Soc. d'Arcueil **2**, 143–158 (1809).
3. D. Brewster, "On the laws which regulate the polarisation of light by reflexion from transparent bodies," Philos. Trans. R. Soc. **105**, 125–159 (1815).
4. A. J. Fresnel, *Mémoire sur la loi des modifications que la réflexion imprime à la lumière polarisée* (De l'Imprimerie De Firmin Didot Fréres, 1834).
5. C. L. Giles and W. J. Wild, "Brewster angles for magnetic media," Int. J. Infrared Millimeter Waves **6**(3), 187–197 (1985).
6. S. B. Glybovski, S. A. Tretyakov, P. A. Belov, Y. S. Kivshar, and C. R. Simovski, "Metasurfaces: From microwaves to visible," Phys. Rep. **634**, 1–72 (2016).
7. K. Achouri and C. Caloz, "Design, concepts, and applications of electromagnetic metasurfaces," Nanophotonics **7**(6), 1095–1116 (2018).
8. V. S. Asadchy, A. Díaz-Rubio, and S. A. Tretyakov, "Bianisotropic metasurfaces: physics and applications," Nanophotonics **7**(6), 1069–1094 (2018).
9. C. Pfeiffer and A. Grbic, "Bianisotropic metasurfaces for optimal polarization control: Analysis and synthesis," Phys. Rev. Appl. **2**(4), 044011 (2014).
10. V. S. Asadchy, Y. Ra'Di, J. Vehmas, and S. Tretyakov, "Functional metamirrors using bianisotropic elements," Phys. Rev. Lett. **114**(9), 095503 (2015).
11. G. Lavigne, K. Achouri, V. S. Asadchy, S. A. Tretyakov, and C. Caloz, "Susceptibility derivation and experimental demonstration of refracting metasurfaces without spurious diffraction," IEEE Trans. Antennas Propag. **66**(3), 1321–1330 (2018).
12. M. Chen, E. Abdo-Sánchez, A. Epstein, and G. V. Eleftheriades, "Theory, design, and experimental verification of a reflectionless bianisotropic Huygens' metasurface for wide-angle refraction," Phys. Rev. B **97**(12), 125433 (2018).
13. R. Paniagua-Domínguez, Y. F. Yu, A. E. Miroshnichenko, L. A. Krivitsky, Y. H. Fu, V. Valuckas, L. Gonzaga, Y. T. Toh, A. Y. S. Kay, B. Luk'yanchuk, and A. I. Kuznetsov, "Generalized Brewster effect in dielectric metasurfaces," Nat. Commun. **7**(1), 10362 (2016).
14. D. R. Abujetas, J. A. Sanchez-Gil, and J. J. Sáenz, "Generalized brewster effect in high-refractive-index nanorod-based metasurfaces," Opt. Express **26**(24), 31523–31541 (2018).
15. Y. Tamayama, "Brewster effect in metafilms composed of bi-anisotropic split-ring resonators," Opt. Lett. **40**(7), 1382–1385 (2015).
16. S. Yin and J. Qi, "Metagrating-enabled Brewster's angle for arbitrary polarized electromagnetic waves and its manipulation," Opt. Express **27**(13), 18113–18122 (2019).
17. C. Wang, Z. Zhu, W. Cui, Y. Yang, L. Ran, and D. Ye, "All-angle brewster effect observed on a terahertz metasurface," Appl. Phys. Lett. **114**(19), 191902 (2019).
18. A. H. Dorrah, M. Chen, and G. V. Eleftheriades, "Bianisotropic Huygens' metasurface for wideband impedance matching between two dielectric media," IEEE Trans. Antennas Propag. **66**(9), 4729–4742 (2018).
19. G. Lavigne and C. Caloz, "Extending the Brewster effect to arbitrary angle and polarization using bianisotropic metasurfaces," in *2018 IEEE International Symposium on Antennas and Propagation & USNC/URSI National Radio Science Meeting*, (IEEE, 2018), pp. 771–772.
20. K. Achouri, M. A. Salem, and C. Caloz, "General metasurface synthesis based on susceptibility tensors," IEEE Trans. Antennas Propag. **63**(7), 2977–2991 (2015).
21. K. Achouri and C. Caloz, *Electromagnetic Metasurfaces: Theory and Applications* (Wiley-IEEE Press, 2020).
22. C. Caloz, A. Alù, S. Tretyakov, D. Sounas, K. Achouri, and Z.-L. Deck-Léger, "Electromagnetic nonreciprocity," Phys. Rev. Appl. **10**(4), 047001 (2018).
23. J. D. Jackson, *Classical electrodynamics* (American Association of Physics Teachers, 1999).
24. K. Achouri, G. Lavigne, and C. Caloz, "Comparison of two synthesis methods for birefringent metasurfaces," J. Appl. Phys. **120**(23), 235305 (2016).
25. A. E. Olk and D. A. Powell, "Accurate metasurface synthesis incorporating near-field coupling effects," Phys. Rev. Appl. **11**(6), 064007 (2019).
26. R. Alaee, M. Albooyeh, A. Rahimzadegan, M. S. Mirmoosa, Y. S. Kivshar, and C. Rockstuhl, "All-dielectric reciprocal bianisotropic nanoparticles," Phys. Rev. B **92**(24), 245130 (2015).
27. M. Odit, P. Kapitanova, P. Belov, R. Alaee, C. Rockstuhl, and Y. S. Kivshar, "Experimental realisation of all-dielectric bianisotropic metasurfaces," Appl. Phys. Lett. **108**(22), 221903 (2016).